Article

Tryptophan Substitutions at the Lipid-Exposed Transmembrane Segment M4 of *Torpedo californica* Acetylcholine Receptor Govern Channel Gating

Jos A. Lasalde, Shiori Tamamizu, Daniel H. Butler, Cecile Rose T. Vibat, Bronson Hung, and Mark G. McNamee

Biochemistry, **1996**, 35 (45), 14139-14148 • DOI: 10.1021/bi961583l

Tryptophan Substitutions at the Lipid-Exposed Transmembrane Segment M4 of *Torpedo californica* Acetylcholine Receptor Govern Channel Gating

José A. Lasalde, Shiori Tamamizu, Daniel H. Butler, Cecile Rose T. Vibat, Bronson Hung, and Mark G. McNamee*

Section of Molecular and Cellular Biology, Division of Biological Sciences, University of California, Davis, California 95616

Received July 1, 1996; Revised Manuscript Received August 26, 1996[⊗]

ABSTRACT: Our previous amino acid substitutions at the postulated lipid-exposed transmembrane segment M4 of the *Torpedo californica* acetylcholine receptor (AChR) focused on the αC418 position. A tryptophan substitution on the αC418 produced a 3-fold increase in normalized macroscopic response to acetylcholine in voltage-clamped *Xenopus laevis* oocytes (Lee et al., 1994). This result was explained by a 23-fold decrease in the closing rate constant measured from single-channel analysis (Ortiz-Miranda et al., 1996). In this study, we introduce more tryptophan substitutions at different positions of this postulated lipid-exposed segment M4 in order to examine functional consequences at the single-channel level. From a series of amino acid substitutions at αG421, only phenylalanine and tryptophan produced a substantial increase in the open time constant. The lack of response from a tyrosine substitution at the αG421 suggests that the side chain volume is not the main structural element responsible for the effect of tryptophan on the stabilization of the open state of the channel. Three multiple mutants, αC418W/G421A, αC418W/G421W, and αC418W/βC447W, were constructed in order to establish the correlation between the number of lipid-exposed tryptophans and the channel open time constant. The αC418W/G421A double mutant demonstrated that when both previous mutations are combined the open time constant was increased 1.5-fold relative to the αC418W. When the two mutants (αC418W and αG421W) were combined in a single mutation, a functional receptor was expressed and the open time constant of the new double mutant increased to 33.4 ms, an 80-fold increase relative to wild type. Estimations of free energy changes calculated from the rate constant for the opening transition suggest that each tryptophan contributes to the stabilization of the open state of the channel by about 0.8 kcal/mol, and the effect of tryptophan substitutions on the free energy is additive. This result suggests that in the channel gating mechanism of the AChR, each subunit contributes independently to the energy barrier between the open and closed state. At selected positions within the postulated lipid surface of the AChR, tryptophan substitutions could establish hydrophobic and perhaps dipole interactions that may play a dramatic role in the channel gating mechanism.

The nicotinic acetylcholine receptor (AChR) from muscle and electric ray organ is an integral membrane protein comprised of four homologous polypeptide subunits in the stoichiometry of $\alpha_2\beta\gamma\delta$ [for review see Karlin and Akabas (1995), Galzi et al. (1991), Pradier and McNamee (1992), and Unwin (1993)]. A consensus model for the AChR topology obtained from hydrophobicity profiles for protein sequences deduced from cDNA sequences indicates that each subunit contains at least four membrane-spanning regions (MSRs) denoted M1 through M4 with both N- and C-terminals located on the extracellular side (DiPaola et al., 1989). The primary and secondary structure of the MSRs may be crucial for the gating and permeation properties of the channel. Most of the studies that combine pharmacological, biochemical, site-directed mutagenesis, and electrophysiological data on MSRs have focused on M2 (Giraudat et al., 1986, 1987, 1989; Hucho et al., 1986; Imoto et al., 1986, 1988, 1991; Charnet et al., 1990; Pedersen et al., 1992; White & Cohen, 1992; Villaroel & Sakmann, 1992). These studies provide strong evidence that M2 segments from each subunit associate about a central axis to form at least part of the aqueous ion channel. In contrast, the M4 segment is the most hydrophobic and least conserved and has been shown to have the largest contact with lipid (Blanton & Cohen, 1992).

In a search for functional cysteines in the receptor, Li et al. (1992) found that substitution of αCys418 for tryptophan in the M4 region of *Torpedo californica* AChR increased the ACh-induced whole cell current. This result was somewhat unexpected since M4 has been postulated to be located at the protein−lipid interface of the receptor. Single-channel analysis on the αC418W showed a 23-fold increase in open time (Lee et al., 1994) compared to the wild type. This αC418 was shown to be one of the five residues labeled by 3-(trifluoromethyl)-3-(*m*-[^{125}I]iodophenyl)diazirine ([^{125}I]-TID) (Blanton & Cohen, 1992, 1994). Further studies in which other amino acids substitutions were performed at αC418 showed that only tryptophan substitutions in this position were able to produce a dramatic decrease (23-fold) of the channel closing rate (Ortiz-Miranda et al., 1996), and a phenylalanine substitution in that position was able to produce a small increase in the open time constant. The results on the αC418 substitutions raised the following questions: (1) are the observations on the αC418W mutation due to the nature or reactivity of the cysteine itself, or (2) are the effects related to disruption of contacts between subunits, allosteric interactions, or a unique interaction of

* Corresponding author: Tel: (916) 752-6764. FAX: (916) 752-2604. E-mail: mgmcnamee@ucdavis.edu.

[⊗] Abstract published in *Advance ACS Abstracts,* October 1, 1996.

S0006-2960(96)01583-8 CCC: $12.00

the tryptophan side chain at the lipid interface of the receptor?

In order to answer these questions, we extended the mutagesesis experiments to other positions within the M4 of the α and β subunits of the *Torpedo* receptor. A reasonable assumption is that conserved positions are likely to represent subunit contacts while less conserved positions might be oriented to the lipid interface. In this work, we selected a highly conserved position among almost all species of AChR, αG421 and the homologous βG450. Also, a tryptophan substitution on the αC412 position of the *Torpedo* receptor, which was also labeled by [^{125}I]TID (Blanton & Cohen, 1992, 1994), was examined. In addition, we analyzed three multiple-tryptophan substitutions which combine the previous αC418W/βC447W mutations with the αG421W. Multiple-tryptophan substitutions within αC418-G421 produced an additive effect on the increase of the open probability of the channel. This study will focus on the functional effects of tryptophan substitutions at the postulated lipid−protein interface of the *Torpedo* AChR.

MATERIALS AND METHODS

Materials

Enzymes for DNA manipulations were purchased from New England Biolabs (Beverly, MA). Taq DNA polymerase amplification kits were obtained from Perkin Elmer-Cetus (Norwalk, CT). Oligonucleotides for PCR and DNA sequencing were from American Synthesis (Pleasanton, CA).

Mutations on the α Subunit of the Torpedo AChR

The coding region of the α subunit of the *T. californica* AChR was subcloned into the *Hin*dIII and *Eco*RI sites of the pGEM3Z(−) vector obtained from Promega (Madison, WI). Directed mutagenesis of the αG421 was carried out by mismatch amplification using two sequential polymerase chain reactions (Horton & Pease, 1991). Mutagenic primers containing the desired codon replacement extended approximately 11 bases on each side of the mismatched region. Flanking primers were designed to recognize sequences outside the *Bgl*II restriction site in the coding region of the α subunit and the *Eco*RI site on the vector portion of the plasmid. Each PCR reaction contained 100 μL of 50 mM KCl, 10 mM Tris-HCl (pH 8.3), 1.5 mM $MgCl_2$, 0.01% gelatin, 200 μM of each deoxynucleotide, 100 ng of DNA template, 1.0 μg of each primer, and 2.0 units of Taq DNA polymerase. Amplification reactions were performed in a DNA thermal cycler (Perkin Elmer-Cetus) programmed for 30 cycles of a three-step protocol: 1 min at 94 °C, 3 min at 48 C, and 3 min at 72 °C. The desired PCR products were purified from excised gel slices with Gene-Clean (Bio101, La Jolla, CA). These DNA fragments were used in a second PCR reaction to generate the fusion product. The 1.3 kb fusion product was purified from the agarose gel with Gene-Clean and digested with *Bgl*II and *Eco*RI. After digestion, the 0.9 kb mutagenized fragment was inserted into the α subunit gene using T4 ligase (Boehringer Mannheim Biochemicals, Indianapolis, IN). The inserts were sequenced using the Sequenase 2.0 kit (United States Biochemical Corp., Cleveland, OH). For the construction of double mutations on the α subunit the αC418W mutation was used as a template.

Mutations on the β Subunit of the Torpedo AChR

The coding region of the β subunit of the *T. californica* AChR was subcloned into the *Eco*RI site of the pSP70 vector from Promega (Madison, WI). Directed mutagenesis of the βG450 position was carried out as described in the previous section for the α subunit mutation. The inserts containing the mutations were ligated into the *Bst*XI and *Eco*RV sites.

In Vitro RNA Transcript Synthesis and Expression in Xenopus laevis Oocytes

Plasmids containing the genes for the α, β, γ, and δ subunits of *Torpedo* AChR were linearized by restriction digestion and used as templates for SP6 mediated *in vitro* transcription (Pradier et al., 1989). Transcription was carried out in the presence of the cap analog m7G(5′)ppp(5′)G, 5′ 7-methylguanosine. Purification of RNA transcripts was performed using Select-D(RF) columns (5 Prime-3 Prime Inc., Boulder, CO). Ovarian lobes were obtained from female *X. laevis*. Follicle cell layers were removed by incubation of the oocytes in Ca^{2+}-free OR2 buffer containing 82.5 mM NaCl, 2.5 mM KCl, 1 mM $MgCl_2$,1 mM Na_2HPO_4, and 5 mM HEPES, pH 7.6, plus 2 mg of collagenase mL (Type 1A, Sigma Chemical Co., St. Louis, MO) for 20 min at room temperature under slow agitation (80−100 rpm) followed by manual defolliculation. Oocytes of stage V and VI were chosen for injection. 50 nL of mRNA subunit transcripts of *Torpedo* AChR (at a concentration of 0.4 ng/nL) was injected into the cytoplasm of *Xenopus* oocytes at a α:β:γ:δ ratio of 2:1:1:1.

Electrophysiological Procedures

Voltage Clamp. Voltage clamp analysis was performed on oocytes 48−96 h after injection. Oocytes were transferred to a 200 μL recording chamber and continuously perfused at a rate of 15 mL/min with MOR2 buffer (82 mM NaCl, 2.5 mM KCl, 1 mM Na_2 HPO_4, 5 mM $MgCl_2$, 0.2 mM $CaCl_2$, and 5 mM HEPES, pH 7.4) containing 2 μM atropine. Acetylcholine solutions used to generate dose−response data were prepared with MOR2 buffer. Oocytes expressing AChR were perfused for 15 s with the agonist solution. For the collection of normalized response data, $CaCl_2$ was excluded and 0.1 mM EGTA was added to minimize the effects of Ca^{2+}-dependent Cl^- current. Voltage and current electrodes were prepared to exhibit resistances of 5−20 and >1 MΩ, respectively. Each oocyte was held at a membrane potential of −100 mV by an Axoclamp 2A two-electrode voltage clamp (Axon Instruments, Buringame, CA). Membrane currents were digitized at 0.5−2 kHz and filtered at 0.1 kHz by an Axon TL-1 interface (Axon Instruments) and recorded by SCAN software (Dagan Corp., Minneapolis, MN) running on an 80386-based computer. SCAN and Inplot (Graphpad Software, San Diego, CA) software were utilized for data analysis. Dose−response data was collected from peak currents at nine ACh concentrations (0.1−1000 μM). The data were fitted using a curve of the form $Y = 100/(1 + (EC_{50}/A)^n)$ and nonlinear regression curves. The EC_{50} and Hill coefficient values for individual oocytes were averaged to generate final estimates. The normalized whole-oocyte currents were analyzed by the unpaired *t*-test from the program Instat (GraphPAD Software, San Diego, CA) to determine if the differences were statistically significant.

Single-Channel Recording. Oocytes expressing the *Torpedo* wild type AChR and mutants were transferred to a hypertonic solution (150 mM NaCl, 2 mM KCl, 5 mM HEPES, and 3% sucrose, pH 7.6) for 20 min in order to induce osmotic shrinkage. After the vitelline membrane was removed manually, the oocytes were placed into a recording chamber and constantly perfused with bath solution (100 mM KCl, 1.0 mM $MgCl_2$, 10 mM HEPES, pH 7.2) at 18 °C. The patch pipets were constructed of Sutter thick-walled borosilicate glass (Sutter Instruments, Novato, CA) and were pulled to exhibit resistances of 8−12 MΩ. The pipet solution contained 100 mM KCl, 10 mM HEPES, 10 mM EGTA, pH 7.2, and 4−50 μM ACh in the cell attached configuration (Hamill et al., 1981). After the gigaohm seal formation (>10 GΩ), the chamber was set to 18 ± 1 °C by adjusting a flow of ice water circulation. The temperature was monitored using a thermocouple (400 series Probe, YSI, Yellow Springs, OH) placed inside the chamber. A DAGAN 3900 (Minneapolis, MN) with a 10 GΩ headstage resistor was used to amplify the channel currents and filter 5−10 KHz (−3 dB; 8-pole Bessel) and stored on a digital data recorder (94 kHz sampling; Instrutech VR-10, Mineola, NY).

Single Channel Analysis. Data were played back into an 80486-based computer through a TL-1 DMA digital interface (Axon Instruments, Foster City, CA) as an analog signal with a sampling of 20 μs (FETCHEX; Axon Instruments, Foster City, CA). Records were digitally filtered (Gaussian low-pass filter: net effective frequency, 4−7 kHz), and single-channel currents were detected with a half-amplitude crossing algorithm (IPROC3; Sachs et al., 1982). The kinetics of expressed AChR are heterogeneous (Naranjo & Brehm, 1993), thus for each patch a subset of apparently homogeneous currents with similar activation characteristics were selected. A homogeneous set of burst was selected using LPROC software (Neil et al., 1991). The list of bursts was further analyzed according to the following criteria: mean amplitude, number of intervals, mean open interval duration, and probability of being open. The ranges used for each of these parameters were estimated by examining the means and the variances for the entire record. This selection procedure reduced the contribution of currents from dissimilar conductance and kinetic forms of cholinergic receptor (Auerbach & Lingle, 1986). After a subset of bursts was selected, a list of open and closed intervals within those bursts was performed and their respective distributions were fitted by a nonlinear least-squares algorithm in which the integral of the exponential probability density function was evaluated over each bin. For the open time analysis we fitted a log bin with of all the open intervals durations (Sigworth & Sine, 1987). The curve fitting for the generated histogram was performed using PSTAT (PCLAMP 6, Axon Instruments, Foster City, CA).

Radioligand Binding Assay

To determine the surface expression levels of AChRs, a radioligand binding assay was performed as described by Li et al. (1990). Immediately following voltage clamping, oocytes were incubated in 80 μL of 10 nM α-bungarotoxin (Amersham Life Sciences, Arlington Heights, IL; ∼74 TBq/nmol) and 0.5 mg of bovine serum albumin/mL in MOR2 for 1.5 h. The excess toxin was removed by washing 5 times with 4 mL of MOR2. The oocytes were transferred into vials containing CytoScint (ICN, Costa Mesa, CA), and β emissions were detected in a liquid scintillation counter (Packard Tricarb 1500). Non-injected oocytes were used as a background for nonspecific binding. A standard curve was obtained by counting 0−20 μL of 1 nM [^{125}I]-α-bungarotoxin (α-BTX) solution (equivalent to 0−20 fmol). Using this approach, we estimated the normalized channel response to ACh. This is defined as the peak of the ACh-induced current (nA) per fmol of surface α-BTX binding sites.

RESULTS

Our previous amino acid substitutions on the *Torpedo* M4 focused on the αC418 position. The αC418W mutants showed a 3-fold increase in normalized macroscopic response to ACh in voltage-clamped *X. laevis* oocytes (Lee et al., 1994). This increased macroscopic response correlated with a 23-fold increase in the open time constant. To further characterize structural and functional changes of the M4 transmembrane domain, a new series of mutations were introduced at other conserved positions of the *Torpedo* M4: αG421, βG450, and βC447. Five amino acid substitutions (A, S, Y, F, and W) made at the αG421, three mutations at the homologous glycine on the β subunit βG450 (W, F, and A), and three multiple mutations combining the previous positions, αC418W/G421A, αC418W/G421W, and αC418W/βC447W, were analyzed in the present study. All of these mutations were carried out using site-directed mutagenesis and DNA sequencing was used to confirm the entire sequence (see Materials and Methods). The maximum ACh-induced currents were recorded at 300 μM ACh, and the maximum channel activity was normalized to the number of α-BTX binding sites on the cell surface.

The relative position of the mutated residue on αM4 to the ion channel or bilayer center may influence channel function. Another residue labeled by [^{125}I]TID and presumably exposed to the lipid interface is the αC412 (Blanton & Cohen, 1992). A tryptophan substitution was constructed in this position in order to compare the results with the αC418W mutant. The normalized response obtained from voltage-clamped oocytes was 313 nA/fmol, which was similar to the wild type response. Single-channel data did not show any significant difference between the αC412W and wild type. This result demonstrated that the alteration of the channel function observed for the αC418W was not necessarily specific to a cysteine side chain.

Figure 1 shows single-current traces for a series of six mutations at the αG421 position. Single-channel currents of the αG421 series of mutants (wild type, A, S, Y, F, and W) were recorded at 18 ± 1 °C, 5 kHz, in the cell attached configuration with a 4.0 μM ACh concentration in the pipet. None of these mutants affected conductance or reversal potential. The conductance of the wild type was 69 ± 3 pS (n = 18 patches, on 12 batches of oocytes) and 71 ± 4 pS (n = 15, on 12 batches of oocytes) for the αG421W. The wild type showed a mean open time of 0.42 ± 0.01 ms (1470 events, n = 10, on five batches of oocytes). The alanine, serine, and tyrosine mutations did not produce any significant effect on the channel open times: G421A, mean open time = 0.44 ± 0.02 (674 events, n = 8, on five batches of oocytes); G421S, mean open time = 0.48 ms ± 0.04 ms (642 events, n = 8, on six batches of oocytes); G421Y, mean open time 0.33 ms ± 0.02 ms (1691 events events, n = 7, on five batches of oocytes). The αG421F showed two time

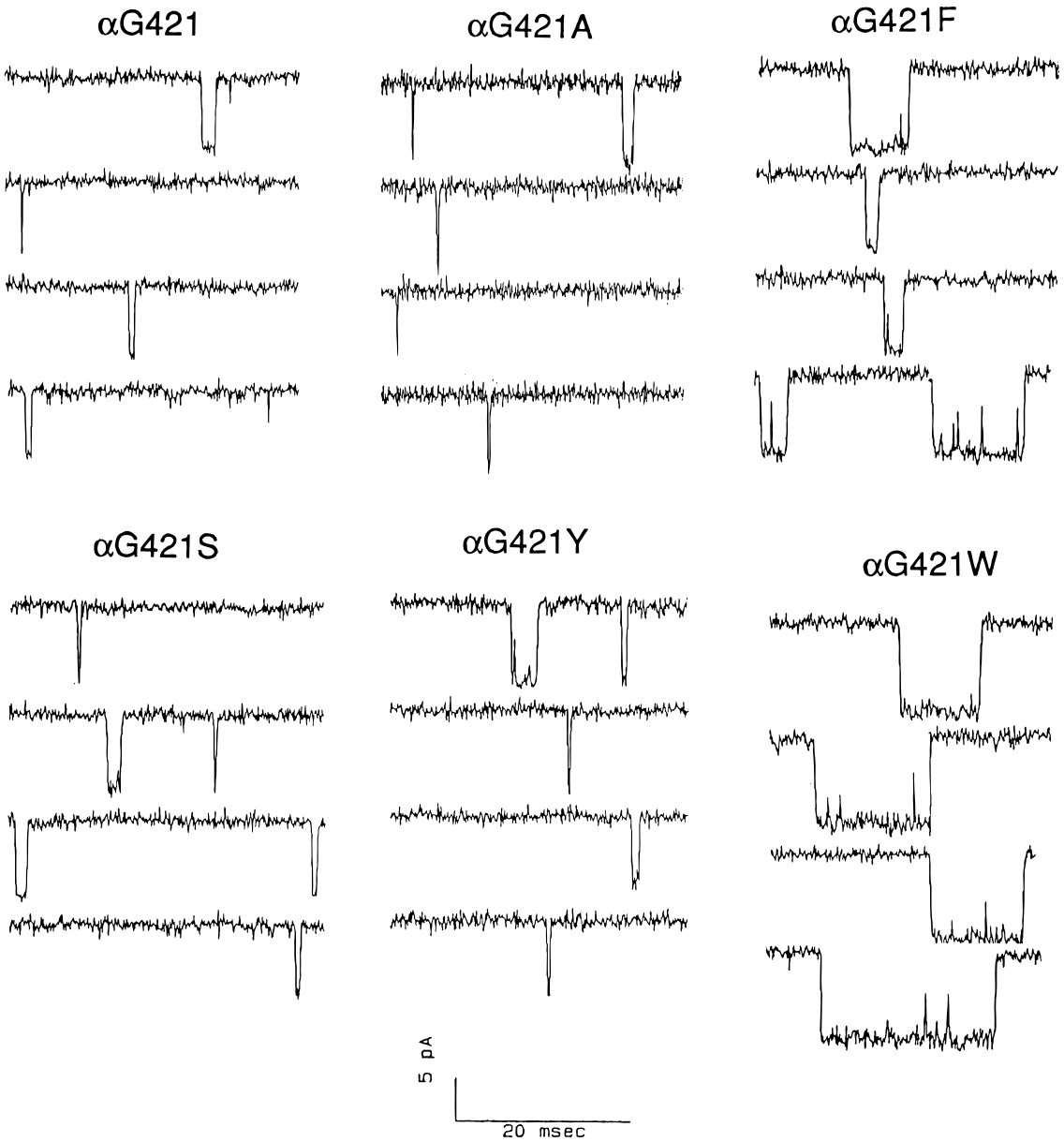

FIGURE 1: Single-channel traces for six amino acid substitutions at the αG421. Recordings were performed in the cell-attached patch configuration at −100 mV, 4 μM ACh, and 18 °C, 5 kHz. Phenylalanine and tryptophan substitutions were the only mutations that increased the open time constant relative to wild type.

constants, and the mean open times and relative areas (α) were as follows: $\tau_1 = 0.43 \pm 0.7$ ms, $\alpha = 0.858$, and $\tau_2 = 3.13 \pm 0.4$ ms, $\alpha = 0.146$ (1116 events, $n = 10$, on 4 batches of oocytes). The longer open time represents an 8-fold increase relative to wild type. This mutant did not produce a significant change in the macroscopic normalized response to ACh. The αG421W showed also two time constants, and the mean open time and relative area were $\tau_1 = 0.954 \pm 0.1$ ms, $\alpha = 0.669$, and $\tau_1 = 3.34 \pm 0.33$ ms, $\alpha = 0.331$ (10 016 events, $n = 12$, on five batches of oocytes; see Figure 3A). The second time constant showed a 12-fold increase in open time constant at 4 μM ACh without affecting the macroscopic current induced by 300 μM ACh. These results correlate with the previous results in the αC418 position where W and F substitutions increased the open time constant. We examined the single-channel currents for three mutations equivalent to αG421 on the β subunit (βG450). The time constants for the these substitutions (βG450A, βG450F, and βG450W) showed the same characteristics as wild type (0.4−1.0 ms), with the tryptophan substitution showing a slight increase in the open time constant. We demonstrated that bulky hydrophobic substitutions like F and W on the αG421 exhibit a similar effect compared to the αC418 position. However, the magnitude of the effect produced by F and W on the open time constant in the αG421 position is slightly smaller compared to that of the αC418 position. Again, this result suggests that there are some specific positions within the αM4 of the *Torpedo* AChR that exhibit a dramatic sensitivity to the channel gating mechanism when the structural perturbation is caused by introduction of a phenyalanine or tryptophan side chains.

Figure 2 shows dose−response curves for wild type and each of the αG421 mutants in the same batch of oocytes. The αG421A and the αG421Y were the only mutants that produced a slight increase in the normalized macroscopic response relative to wild type from 10 to 300 μM ACh. This result was unexpected since the kinetic behavior of this mutant was similar to wild type (see Table 2). The αG421S,

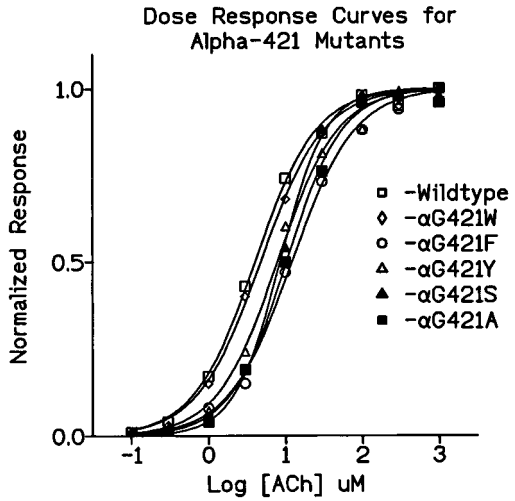

FIGURE 2: Dose−response curves for the αG421 voltage-clamped oocytes. Data points from all ACh concentrations were fitted with the Hill equation, $Y = 100/[1 + (K_d/A)^h]$. Peak activity from individual oocytes was obtained from ACh-induced current at 1.0, 10, 30, 100, 300, and 1000 μM ACh. The values at each concentration were averaged, and dose−response curves were reconstructed and normalized to the maximum response.

Table 1: Functional Effects of *Torpedo* M4 Mutations

Torpedo M4 mutants[a]	EC50 (mM)	Hill coefficient[b]	normalized response[c] (nA/fmol)
wild type	4.2 ± 2.2	1.21 ± 0.1	282 ± 62
αG421 mutants			
αG421W	2.9 ± 0.4	1.1 ± 0.1	166 ± 44
αG 421F	8.5 ± 6.0	1.2 ± 0.1	182 ± 24
αG421Y	4.5 ± 2.8	1.3 ± 0.4	272 ± 82
αG421S	8.7 ± 2.8	1.5 ± 0.4	197 ± 85
αG421A	8.6 ± 3.8	1.3 ± 0.3	387 ± 153
βG450 mutants			
βG450W	3.9 ± 1.5	1.6 ± 0.2	278 ± 74
βG450F	4.4 ± 1.9	1.6 ± 0.6	197 ± 34
βG450A	7.7 ± 3.6	1.6 ± 0.3	271 ± 87
αC412W	3.5 ± 3.0	1.5 ± 0.2	313 ± 146

[a] 8−15 oocytes tested for each mutation. [b] Data points from all ACh concentrations were fitted with the Hill equation, $Y = 100/[1 + (K_d/A)^h]$. [c] Normalized peak activity for each oocyte was obtained from ACh-induced current at 300 μM ACh divided by a number of surface α-bungarotoxin binding sites on the same oocyte.

αG421F, and αG421W did not show any significant difference from wild type in all the concentration ranges tested (0.10−300 μM ACh). Table 1 shows the data extracted from dose−response relationships for the αG421 and β6450 mutations which include EC_{50} values, Hill coefficients, and normalized responses to 300 μM ACh. Normalized responses were obtained by measuring the currents elicited by 300 μM ACh (only one current measured per oocyte; 10−30 oocytes per mutation were used) and estimating the fmol of toxin binding sites per individual oocyte tested. None of the mutants showed alterations in the expression levels in the toxin assay. Hill coefficients and EC_{50} values for each dose−response curve were calculated as described in Materials and Methods. The Hill coefficients of the mutants shown on Table 1 are not significantly different from the typical wild type value of 1.2, indicating that these mutants did not produce a significant effect on cooperativity. The EC_{50} ranges for all the mutants (2.9−8.7 μM) were similar to wild type (4.2 μM). Although there was not a significant difference between the EC_{50} values, this does not prove that the ACh binding was not affected since this ligand binding could be affected by the opening and closing rate constants and also the rate of desensitization (Colquhoun & Odgen, 1988).

Table 2: Functional Consequences of Multiple M4 Mutations[a]

AChR type	EC50 (μM)	Hill coefficient[b]	normalized response[c] (nA/fmol)
wild type (10)	9.8 ± 5.2	1.4 ± 0.2	279 ± 111
αC418W (6)	2.5 ± 0.4	1.2 ± 0.1	638 ± 138
αC418W/G421A (6)	5.4 ± 0.6	1.4 ± 0.1	3822 ± 1425
αC418W/βC447W (6)	3.0 ± 1.7	1.4 ± 0.1	980 ± 371
αC418W/G421W (8)	2.9 ± 1.8	1.3 ± 0.1	1244 ± 304

[a] Values ± SD are given. Number in parentheses indicates the number of oocytes tested. [b] Data points from all ACh concentrations were fitted with the Hill equation, $Y = 100/[1 + (K_d/A)^h]$. [c] Normalized peak activity for each oocyte was obtained from ACh-induced current at 300 μM ACh divided by a number of surface α-bungarotoxin binding sites on the same oocyte.

The multiple mutations αC418W/G421A, αC418W/βC447W, and αC418W/G421W showed significant increases in the normalized response to ACh when compared to the αC418W and the αG421W (see Table 2). The relative order of normalized responses to 300 μM ACh of the M4 mutations is wild type ≪ αG421W < αC418W < αC418W/G421A < αC418W/βC447W < αC418W/G421W.

The combined double mutant αC418W/G421A produced an increase in the open time constant relative to αC418 W. This αC418W/G421A double mutant was constructed to extend the previous results obtained for the αC421A (2-fold increase in the macroscopic response to ACh). An alanine substitution (αG421A) at the αC418W mutant also produced an additive effect on the open time constant of the channel. Figure 4A shows single-channel traces and an open time histogram for the αC418W/G421A double mutant at −100 mV and 18 °C. The mean open time for this double mutant was 14.86 ± 0.32 ms (14 407 events, $n = 5$). This small perturbation induced by a substitution of alanine to glycine at the α6421 position produced an increase in the open time constant of the previous αC418W mutant (9.8 ms, see Figure 3B). This result confirms the sensitivity of this region (αC418-G421) to structural perturbations.

Another multiple tryptophan substitution was the αC418W/βC447W, which combined the αC418 and the equivalent position in the β-subunit C447. Figure 4B shows single-channel traces for this multiple-tryptophan substitution. The open time constant for this mutant was 22.5 ms. This value represents a 54-fold increase in the open time constant when compared to wild type. When the two previous mutations, αC418W and αG421W, were combined in the α subunit, a functional receptor was expressed and a much more dramatic increase in the open time constant was produced. The αC418W/G421W resulted in an 84-fold increase in the open time compared to the wild type. Figure 4C shows single-channel traces and open time histogram for the αC418W/G421W double mutant at −100 mV and 18 °C. The mean open time for this double mutant was 33.34 ± 0.82 ms, $n =$ 3 patches, 2 053 events. Again, these results further demonstrate that bulky aromatic substitutions within the αC418-G421 of the *Torpedo* α subunit produce an additive effect on the open time constant of the channel. An 80-fold increase in the open time constant relative to the wild type could be considered a very dramatic increase in the open

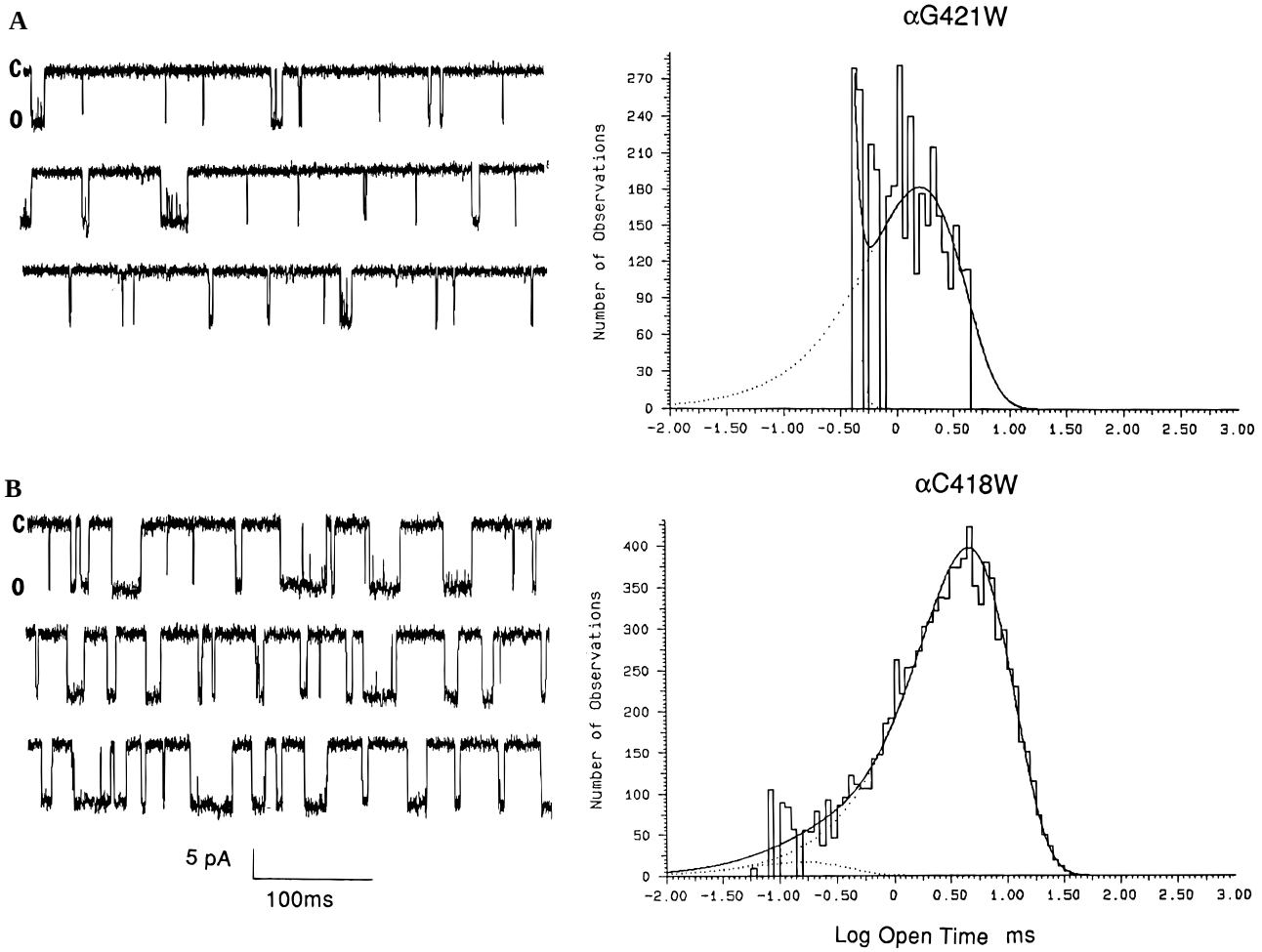

FIGURE 3: Single-channel currents of AChRs containing the αG421W and αC418W mutants expressed in *Xenopus* oocytes. (Left) Single-channel currents elicited by 4 μM ACh. The membrane potential was −100 mV, 18 °C, and the Gaussian filter was set at 10 kHz. (Right) Open time duration histograms corresponding to the traces on the left. The curves are sums of exponentials with the following fitted parameters: (A) αG421W, τ_{o1} = 1.27 ms, and τ_{o2} = 4.29 ms, total number of events is 10 016. The fast component is 0.42 ms, which is close to wild type. (B) αC418W, τ_o 4.6 ms, total number of events is 14 724.

channel probability. In addition, this result suggests that two bulky hydrophobic residues could be accommodated within the αC418 and αG421 positions without loss of receptor expression or function.

DISCUSSION

Among the four postulated transmembrane domains of the *T. californica* AChR, M4 is the most hydrophobic and has the lowest level of side chain conservation. The M4 transmembrane segment has been proposed to have the largest contact with lipids (Blanton & Cohen, 1992, 1994) and is not believed to be part of the ion channel or binding site for ACh. The finding that showed that a single mutation at the postulated protein−lipid surface of the AChR could produce such dramatic effects on the closing transition of the channel (Lee et al., 1994) raised some questions regarding a possible role of the lipid-exposed region on the gating mechanism. Numerous studies of lipid effects on the AChR structure and function have demonstrated that membrane lipid composition can modulate the receptor function (Fong & McNamee, 1987; Pradier & McNamee, 1992; Bhushan & McNamee, 1993; Lasalde et al., 1995a).

A recent extension of our studies on the αM4 of the *Torpedo* AChR, focusing on a kinetic analysis of the αC418W mutant, demonstrates that the tryptophan substitution at this particular lipid-exposed residue produces significant effects on the channel gating kinetics (Lee et al., 1994). A burst analysis of the αC418W performed over a range of ACh concentrations demonstrated that the key factor that increased open channel probability of this mutant was a 23-fold decrease in the closing rate (Ortiz-Miranda et al., 1996). These results further supported a possible role of a portion of the *Torpedo* αM4 region on the channel gating mechanism. Our next step toward defining a mechanism by which bulky aromatic residues produce such an effect on the AChR channel gating was directed to answer the following questions: (1) Are these effects exclusive to Cys residues or can they be detected in other residues within the M4 transmembrane segment? (2) Are the observed effects on the C418W exclusive to an isolated residue or a cluster or residues within the αM4? (3) Can these effects be amplified by increasing the number of aromatic hydrophobic groups in a specific sensitive region of the M4?

The main experimental result in this work is the additive effect on the prolonged open time constant caused by the increase in the number of tryptophan substitutions at the αC418, βC447, and αG421 positions of the postulated lipid-exposed transmembrane segment M4. A normalized open time histogram for five multiple tryptophan mutations is shown in Figure 5A. A correlation of the open time and

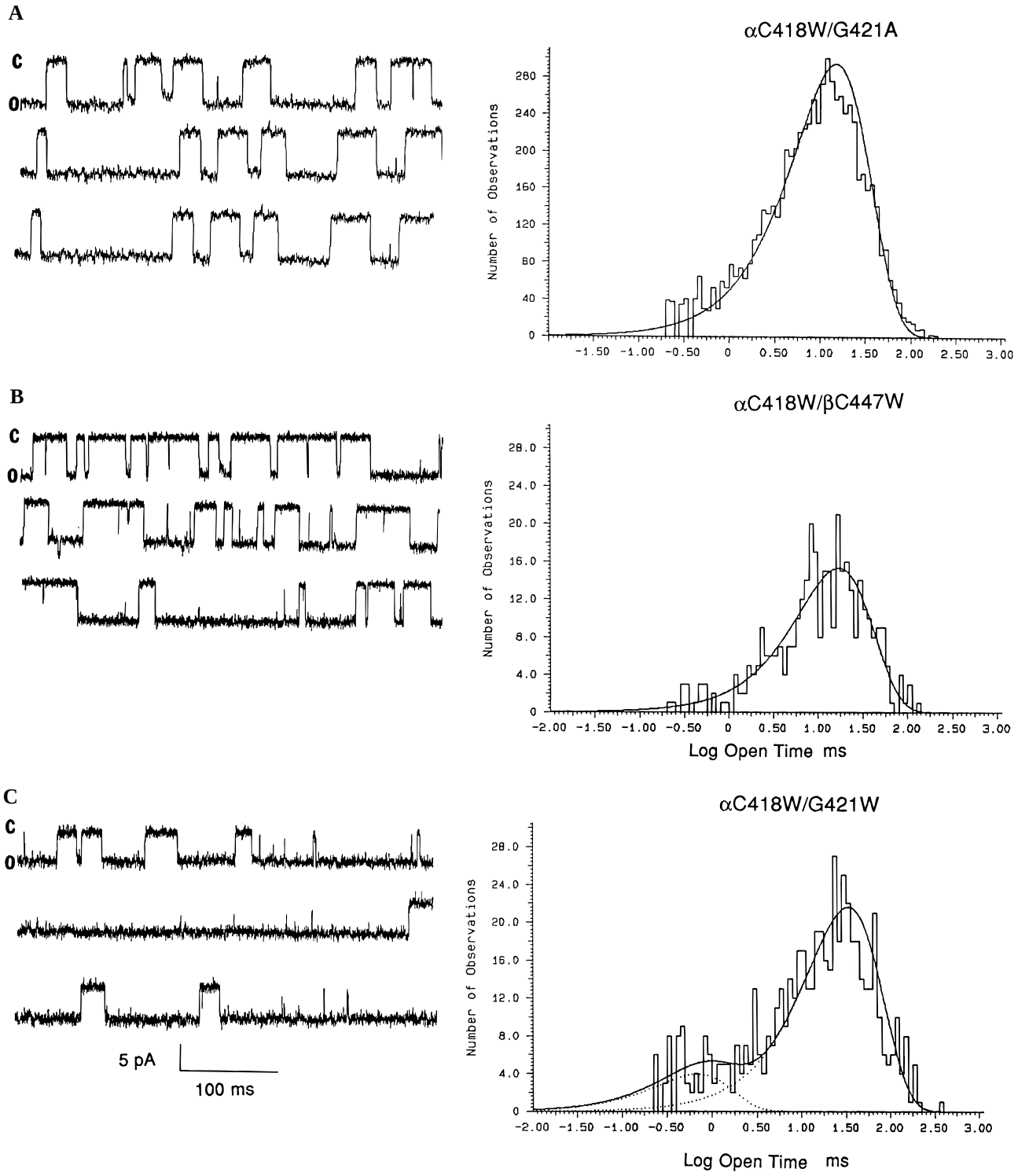

FIGURE 4: Single-channel traces of AChRs containing the αC418W/G421A (A), αC418W/βC447W (B), and αC418W/G421W (C) mutants expressed in *Xenopus* oocytes. (Left) Single-channel currents elicited by 4 μM ACh. The membrane potential was −100 mV, 18 °C, and the Gaussian filter was set at 5 kHz. (Right) Open time duration histograms corresponding to the traces on the left. The curves are sums of exponentials with the following fitted parameters: αC418W/G421A, τ_o = 14.9 ms, total number of events is 14 407; αC418W/βC447W, τ_o = 17.1 ms, total number of events is 5040. αC418W/G421W, τ_o = 33.3 ms, total number of events is 2053.

the increase in the hydrophobicity index caused by the number of substituted tryptophans is shown in Figure 5B. This result suggests a possible linear correlation between the open probability of the channel and the number of substituted tryptophans.

To simplify our results, we use three simple kinetic equations that can describe the different classes of openings that we observe for these mutations:

$$\mathrm{O1} \underset{a_1}{\longrightarrow} \mathrm{C} \tag{1}$$

$$\mathrm{O1} \underset{a_1}{\longrightarrow} \mathrm{C} \underset{a_2}{\longleftarrow} \mathrm{O2} \underset{a_i}{\longrightarrow} \mathrm{I} \tag{2}$$

$$\mathrm{C} \underset{a_3}{\longleftarrow} \mathrm{O3} \underset{a_i}{\longrightarrow} \mathrm{I} \tag{3}$$

where C represents a collection of possible closed states, O1 is the less stable open state that represents the wild type

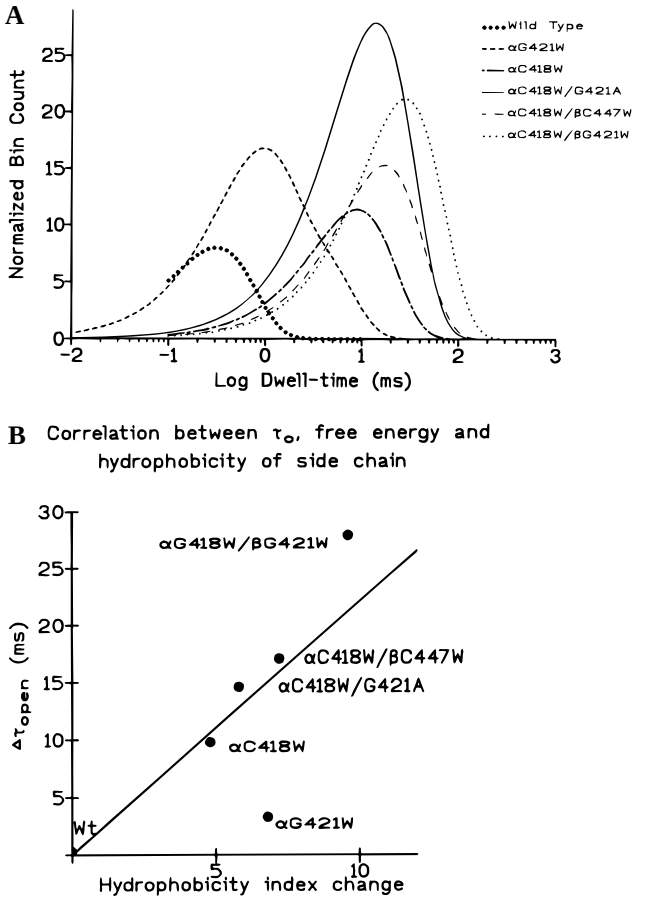

FIGURE 5: (A) Normalized histogram for the open time durations for all the multiple-tryptophan substitutions on the *Torpedo* M4. As shown, the order of increased open time estimated at 4.0 μM ACh relative to wild type is αG421W < αC418W < αC418W/G421A < αC418W/βC447W < αC418W/G421W (33 ms). (B) Correlation of open time and net hydrophobicity index calculated by adding the individual hydrophobicity index change per substitution.

open conformation ($t_{open} = 400-500$ μs) and some mutants, such as αG421A, αG421S, βG450A, βG450F, βG450W, and αC412W. O2 represents a second and slightly more stable open conformation present in the αG421F, αC418F, and αG421W mutants ($t_{open} = 2-5$ ms). These mutations have both O1 and O2 types of open conformations which means that they retain characteristics of the wild type (eq 2). The third open state O3 represents mutations in which the O1 conformation is barely detected (or less than 3% of the events), indicating that a more dramatic change in conformation has produced a very stable open state ($t_{open} > 10$ ms) (eq 3). This O3 state is represented by αC418W, αC418W/G421W, αC418W/G421A, and C418W/βC447W. The I state is an interrupted state (brief closures) that is present in both O2 and O3 states. These interruptions or gaps have been studied in BC3H-1 cells (Sine & Steinbach, 1986) and are kinetically distinct from longer closures which separate channel openings. In this paper, we focus only on the open time constant (or closing rate). Although the gaps provide information on the opening rate, we have used burst analysis to demonstrated that the main effect on the αC418W is due to a decrease in the closing rate (Ortiz-Miranda et al., 1996). The rate constants a_1, a_2, and a_3 are the inverse of the time constant τ for each activation step and f (fraction of brief activations for state O1). Also, the rate of interruptions a_i can be estimated from the inverse of time constant for the interruptions τ_i. In eq 2, the fraction of O1/O2 openings is f; this is also estimated also from the single-channel data.

Table 3: Correlation between the Time Constant and Free Energy for the O2 and O3 Open States[a]

mutation	transition type	τ	U (kcal/mol)
αG421F	O2 → C	3.13 ms	−1.237
αC418F	O2 → C	3.82 ms	−1.323
αG421W	O2 → C	4.29 ms	−1.393
αC418W	O3 → C	9.81 ms	−1.889
αC418W/G421A	O3 → C	14.9 ms	−2.140
αC418W/βC447W	O3 → C	22.5 ms	−2.387
αC418W/G421W	O3 → C	33.3 ms	−2.623

[a] t_n for wild type is 0.42 ms at −100 mV and 18 °C.

For the states in eqs 1−3, the absolute rate theory provides a correlation between the rate constant and the energy barrier (U_n) that the ion channel must overcome to make a transition where K is the Boltzmann constant and T is the absolute temperature (eqs 4 and 5).

$$a_n \approx \exp(-U_n/\mathrm{K}T) \quad (4)$$

$$U_n = \mathrm{K}T \ln(a_n) \quad (5)$$

For example, U_1 represents in our scheme the difference in energy between the open state O1 and the transition state that leads to channel closure. We estimated the transition energy between the O1 → C, O2 → C, and O3 → C states. The energy difference can be estimated from eq 6:

$$U = RT \ln(a_o/a_n) \quad (6)$$

where a_o and a_n are the rates before and after the amino acid substitution. Table 3 shows some transition energies for a list of M4 AChR mutations.

The energy barrier between the O2 → C states is about −1.4 kcal/mol, and O3 → C transitions are on the order of −2.623 kcal/mol. The stabilization of the open state estimated from the transition energy for the αC418 and βC447 position is about −0.8 kcal/mol per tryptophan substitution and about −0.7 kcal for the αC421W. This additive effect of the αC418 and βC447 tryptophan substitutions on the energy barrier for the open state transition suggest that this effect could be related to the gating mechanism of the channel. The range of energy differences for these transitions is compatible with Van der Waal's bond energy. The Van der Waal's energy becomes significant when numerous atoms in one of a pair of molecules can simultaneously come close to many atoms of the other. This implies that effective Van der Waal's interactions depend on steric complementarity. The question is how and why bulky hydrophobic amino acid side chains produce such changes in the energy barrier for the open state of the channel though the recruitment of Van der Waal's interactions. Is the volume of the substituted residue a key factor? Differences observed between the αG421Y and the αG421F may point towards the answer. The volume occupied by these residues inside a protein is very similar: Y is 203.6 Å^3, and F is 203.4 Å^3 (Chothia, 1975). The αG421Y mutation did not produce the O2 → C transition, suggesting that the polarity of the hydroxyl group rather than the volume occupied by the residue was critical. If polar groups could not establish appropriate interactions, the observed effects could be due to penetration of phenylalanine and tryptophan

groups into the membrane lipid interface. Another possible scenario is that the substituted residue causes a disruption of allosteric contacts between M1 or M3, indirectly affecting M2. If this were the case the penetration volume or radius of the residue could be critical. This, however, does not seem to be the case since Y with about the same penetration radius was F (∼4.0 Å) did not produce any significant effect on the energy barrier of the open channel state. Using the dimensions obtained from Unwin's structure at 9 Å resolution (Unwin, 1993) the center-to-center distances between neighboring subunits at the bilayer center are 12 and 20 Å at the surface. Thus, at the bilayer center the transmembrane segments are packed at about $2\pi 6^2 Å^2/4$, giving an approximate area of 56 $Å^2$ per segment and a radius of 3 Å. Assuming an α helical structure for M4, αC418 is located at the center of the bilayer. It seems unlikely that a tryptophan with a diameter of about 8.4 Å could be accommodated between such tightly packed subunits. The strongest evidence that this residue is lipid exposed is the result of photoaffinity labeling by Blanton and Cohen (1992; 1994).

The lack of effect observed on another lipid-exposed mutant, αC412W, clearly suggests that the αC418W observation is not exclusive to cysteine residues or to a lipid-exposed residue. This could indicate that the region between αC418 and αG421 may participate in the gating of the channel through a long-range mechanism that remains to be determined. Examining the structural information available on the open state of the channel provided by Unwin (1995), it is interesting that both α subunits have a rotation of about 3.9 degrees in clockwise orientation relative of the ion pore or the M2 transmembrane segments. This could explain the lack of response for the αC412W which may be located below the gate level if an α-helical structure is assumed. The observed effects on these sensitive positions could possibly be related to residues that display considerable motion during the active cycle of the closed to open isomerization of the intermembrane segments. This rotation transmitted from the binding sites though the structure in the membrane by the α subunits seems to be diminished below the center of the bilayer, where little if any considerable motion was detected (Unwin, 1995).

It is also possible to imagine that a lipid-exposed residue may exert "drag" in the bilayer during the active cycle of channel opening. If both residues penetrate the bilayer, then what causes such a dramatic difference between phenyalanine and tryptophan? The cation channel peptide gramicidin, which contains four tryptophan groups at different positions (9, 11, 13, 15), can be used as a model to compare the dynamic differences between these two side chains. The tryptophan side chains in the gramicidin cation channel have been shown to orient the channel with respect to the bilayer (Hu et al., 1993) and also facilitate channel conductance (Becker et al., 1991; Hu & Cross, 1995). Numerous suggestions in the literature have proposed that the tryptophan groups of gramicidin may hydrogen bond to lipids (Meulendijks et al., 1989; O'Connell et al., 1990; Scarlatta, 1991; Lazo et al., 1992; Hu et al., 1993, 1995; Hu & Cross, 1995). A recent study based on ^2H and ^{15}N NMR has shown that the N−H bond and the indole five-membered ring are oriented toward the bilayer surface and the six-membered hydrophobic group is buried in the lipid bilayer (Hu et al., 1995). The suggestion that the dipole moments are important for the facilitation of cation transport has been demonstrated by the use of phenylalaine-substituted gramicidins (Becker et al., 1991). When phenylalanine side chains, which have no dipole moments, are substituted for tryptophan, the conductance rate decreases. The free energy of stabilization of channel conductance due to indole group substitution has been estimated to be about 0.8 kcal/mol (Hu & Cross, 1995). This value is the same as the energy that we calculated from the tryptophan substitution on the lipid-exposed region of the AChR (∼0.8 kcal/mol). The functional importance of dipole moments resulting from the molecular dynamics of indole groups on membrane proteins like ion channels has not been well documented. However, the functional roles of tryptophan in gramicidin could well be reproduced by membrane proteins like the AChR.

The 9 Å structure obtained by micrograph image reconstruction of frozen postsynaptic membranes reported by Unwin (1993) suggests a β-sheet structure for the M1, M3, and M4 based on a lack of similar density profiles at the AChR periphery. On the other hand, biochemical labeling data support an α-helix structure (Blanton & Cohen, 1992, 1994). Recently, a hydrogen/deuterium exchange study using FTIR also suggested an α-helical structure for all four transmembrane segments of *Torpedo* AChR (Baenzinger & Méthot, 1995). Five residues of the *Torpedo* αM4 transmembrane segments were labeled by [^{125}I]TID in an α-helix pattern: αV425, αT422, αC418, αM415, and αC412 (Blanton & Cohen, 1994). Of these residues, the αC418 has been shown to be the most sensitive to hydrophobic aromatic substitutions (Lasalde et al., 1995b). If the M4 transmembrane segment is α-helical, then the tryptophan mutation at the αC418 and βC447 positions will be located at the center of the bilayer. This implies that at the center of the bilayer leaflet a lipid-buried tryptophan may be buried inside the acyl chains near the fatty acid tail-to-tail junction. Perturbation of this junction by an exposed tryptophan could also cause changes of lipid dynamics at the center of the bilayer. This hypothesis needs further experimental support.

It is unlikely that a perturbation induced by a tryptophan substitution from this region of M4 could propagate to the M2 transmembrane segment to produce a significant conformational alteration of the ion pore since the permeation (conductance) properties and the ion selectivity (reversal potential) were not altered. It is important to emphasize that the free energy barrier for the αC418W and βC447W substitutions is additive. This suggests that in the channel gating mechanism of the AChR, each subunit contributes independently to the transition between the open and closed states. From these results it is clear that the relative position of the tryptophan substitution relative to the ion pore and possibly to the bilayer might be a critical factor in determining the degree of perturbation. In addition, this present work suggests that Van der Waal's and perhaps dipole interactions at the periphery of the AChR with the lipid interface could play a significant role in the overall mechanism of channel gating.

REFERENCES

Auerbach, A., & Lingle, C J. (1986) *J. Physiol. 378*, 119−140.

Baenzinger, J. E., & Méthot, N (1995) *J. Biol. Chem. 270* (49), 29129−29137.

Becker, M. D., Greathouse, D. V., Koeppe, R. E., II, & Andersen, O. S. (1991) *Biochemistry 30*, 8830−8839.

Bhushan, A., & McNamee, M. (1993) *Biophys. J. 64*, 716−723.
Blanton, M. P., & Cohen, J. B. (1992) *Biochemistry 31* (15), 3738−3750.
Blanton, M. P., & Cohen, J. B. (1994) *Biochemistry 33* (10), 2859−2872.
Charnet, P., Labarca, C., Leonard, R. J., Vogelaar, N. J., Czyzyk, L., Gouin, A., Davison, N., & Lester, H. A. (1990) *Neuron 4*, 87−95.
Chothia C. (1975) *Nature 254*, 306−308.
Colquhoun, D., & Odgen, D. C. (1988) *J. Physiol. 395*, 131−159.
DiPaola, M., Czajkowski, C., & Karlin, A. (1989) *J. Biol. Chem. 264*, 15457−15463.
Fong, T. M., & McNamee, M. G. (1987) *Biochemistry 26*, 3871−3880.
Galzi, J.-L., Revah, F., Bessis, A., & Changeux, J.-P. (1991) *Annu. Rev. Pharmacol. 31*, 37−72.
Giraudat, J., Dennis, M., Heidmann,T., Chang, J.-Y., & Changeux, J.-P. (1986) *Proc. Natl. Acad. Sci. U.S.A. 83*, 2719−2723.
Giraudat, J., Dennis, M., Heidmann,T., Hamont, P. Y., Lederer, F., & Changeux, J. P. (1987) *Biochemistry 26*, 2410−2418.
Giraudat, J., Gali, J., Revah, F., Changeux, J.-P., Haumont, P., & Lederer, F. (1989) *FEBS Lett. 253*, 190−198.
Hamill, O. P., Marty, A., Neher, E., Sakmann, B., & Sigworth, F. J. (1981) *Pflügers Arch. 391* (2), 85−100.
Horton, R. M., & Pease, L. R. (1991) *Directed Mutagenesis*, pp 217−246, IRL Press, New York.
Hu, W., & Cross, T. A. (1995) *Biochemistry 34*, 14147−14155.
Hu, W., Lee, K. C., & Cross, T. A. (1993) *Biochemistry 32*, 7035−7047.
Hu, W., Lazo N. D., & Cross, T. A. (1995) *Biochemistry 34*, 14138−14146.
Hucho, F., Oberthur, W., & Lottspeich, F. (1986) *FEBS Lett. 205*, 137−142.
Imoto, K., Methfessel, C., Sakmann, B., Mishina, M., Mori, Y., Konno, T., Fukuda, M., Kurasaki, M., Bujo, H., Fujita, Y., & Numa, S. (1986) *Nature 324*, 670−674.
Imoto, K., Busch, C., Sakmannn, B., Mishina, M., Konno, T., Nakai, J., Buho, H., Mori, Y., Fukuda, K., & Numa, S. (1988) *Nature 335*, 665−648.
Imoto, K., Konno, T., Nakai, J., Wang, F., Mishina, M., & Numa, S. (1991) *FEBS Lett. 289*, 193−200.
Karlin, A., & Akabas, M. H. (1995) *Neuron 15*, 1231−1244.
Lasalde, J. A. Colom, A., Resto, E., & Zuazaga, C. (1995a) *Biophys. Biochim. Acta 1235*, 361−368.
Lasalde, J. A., Ortiz-Miranda, Butler, D., Tamamizu, S., Vibat, C. R., Pappone, P., & McNamee M. (1995b) *Biophys. J.*, A233.
Lazo, N. D., Hu, W., & Cross, T. A. (1992) *J. Chem. Soc., Chem. Commun.*, 1529−1531.
Lee, Y.-H., Lasalde, J., Rojas, L., McNamee, M., Ortiz-Miranda, S. I., & Pappone, P. (1994) *Biophys. J. 66*, 646−653.
Li, L., Schuchard, M., Palma, A., Pradier, L., & McNamee, M. G. (1990) *Biochemistry 29*, 5428−5436.
Li, L., Lee, Y. H., Pappone, P., Palma, A., & McNamee, M. G. (1992) *Biophys. J. 62* (1), 61−63.
Meulendijks, G. H. W. M., Sonderkamp, T., Dubois, J. E., Nielen, R. J., Kremers, J.A., & Bucks, H. M. (1989) *Biochim. Biophys. Acta 979*, 321−330.
Naranjo, D., & Brehm, P. (1993) *Science 260*, 1811−1814.
Neil, J., Xiang, Z., & Auerbach, A. (1991) *Methods Neurosci. 4*, 474−490.
O'Connell, A. M., Koeppe, R. E., II, & Andersen, O. S. (1990) *Science 264*, 1256−1259.
Ortiz-Miranda, S., Lasalde, J. A., Papone, P., & McNamee, M. (1996) *Biophys. J.* (submitted).
Pedersen, S. E., Sharp, S. D., Liu, W. S., & Cohen, J. B. (1992) *J. Biol. Chem. 267*, 10489−10499.
Pradier, L., & McNamee, M. G. (1992) *The Structure of Biological Membranes*, pp 1047−1106, Telford, Caldwell, NJ.
Pradier, L., Yee, A. S., & McNamee, M. G. (1989) *Biochemistry 28* (16), 6562−6571.
Sachs, F., Neil, J., & Barkakati, N. (1982) *Pflügers Arch. 395*, 331−340.
Scarlatta, S. F., (1991) *Biochemistry 30*, 9853−9859.
Sigworth, F. J., & Sine, S. M., (1987) *Biophys. J. 52*, 1047−1054.
Sine S. M., & Steinbach, J.,H., (1986) *J. Physiol. 373*, 129−162.
Unwin, N. (1993) *J. Mol. Biol. 229*, 1101−1124.
Unwin, N. (1995) *Nature 373* (5), 37−43.
Villaroel, A., & Sakmann, B. (1992) *Biophys. J. 62*, 196−205.
White, B. H., & Cohen, J. B. (1992) *J Biol. Chem. 267*, 15770−15783.

BI961583L